Discrete implementation of biologically inspired image processing for target detection

Article · December 2011

DOI: 10.1109/ISSNIP.2011.6146617

CITATIONS
8

READS
53

4 authors:

Kerry J. Halupka
IBM Research Australia
7 PUBLICATIONS **27** CITATIONS
SEE PROFILE

Steven D Wiederman
University of Adelaide
38 PUBLICATIONS **340** CITATIONS
SEE PROFILE

Ben Cazzolato
University of Adelaide
271 PUBLICATIONS **2,070** CITATIONS
SEE PROFILE

David O'Carroll
Lund University
142 PUBLICATIONS **2,398** CITATIONS
SEE PROFILE

Discrete Implementation of Biologically Inspired Image Processing for Target Detection

Kerry Halupka [#1], Steven Wiederman [*2], Benjamin Cazzolato [#3], David O'Carroll [*4]

[#] *Faculty of Engineering, Computer and Mathematical Sciences,* [*] *Faculty of Health Sciences,*

The University of Adelaide, Australia

[1] kerry.halupka@adelaide.edu.au

[2] steven.wiederman@adelaide.edu.au

[3] benjamin.cazzolato@adelaide.edu.au

[4] david.ocarroll@adelaide.edu.au

***Abstract*— In nature, systems which visually process the world around them, in computationally efficient manners, have evolved over millions of years. The brain of an insect, which is smaller than a grain of rice, and with less than a million neurons, can effectively engage in computationally challenging tasks. For example, visually detecting and discriminating small moving objects, which are embedded within a complex optical flow pattern (induced by ego-motion). This task has yet to be perfected by current image processing techniques, though recent research is taking inspiration from nature to do so, in creating biologically inspired models of insect vision. This paper presents the progress made on our previous computational model based on electrophysiological data of a class of cells called Small Target Motion Detection neurons (STMDs). This model was based in the continuous temporal domain with constraints imposed on the inputs to the model. Modifications to the model include re-implementation in the discrete domain, the addition of a more physiologically accurate log-normal filter, the inclusion of a Reichardt Correlator and the creation of the highly controllable virtual world as a front end to the model. Model outputs show that the target detecting characteristics of the previous continuous model is maintained, though in a form which is directly applicable to hardware implementation.**

I. Introduction

The task of discerning a target amongst visual 'clutter', often without the presence of relative motion cues, is a task which has been elegantly achieved by flying insects. The multifaceted eye of many insects has a much lower visual resolution than a single lens type eye due to the severe effect of optical diffraction at small lens aperture [1]. Despite this limitation many insects display impressive feats of acrobatic flight during the detection and pursuit of prey, or social interactions with potential mates [2]. Of particular interest to this research is the ability of insects to respond to small moving targets, often without the presence of relative motion cues, against visually cluttered backgrounds [2].

Electrophysiological experiments on flying insects have revealed that certain visual neurons in higher order regions of the brain respond selectively to small moving targets, with the response decreasing with increase in target size [2-4]. These neurons are referred to as Small Target Motion Detection neurons (STMDs). Interestingly, the response of STMD neurons has been found to be robust under a variety of confounding background images, including when the insect is moving relative to the background [4], a situation which is the downfall of many simulated target detection algorithms [5]. Thus, a model which mimics the characteristics of these neurons could provide a new, computationally efficient, means of detecting small moving targets. Our previous work proposed that target motion was computed locally, by 'Elementary Small Target Motion Detector' elements (ESTMDs) and led to successful development of such a model, tuned to detect small objects, of approximately 1°x1°, moving at approximately 100°/s. based largely on the observed physiology of key stages of the fly visual system [6, 7].

While the ESTMD model [6, 7] mimicked several desirable properties of biological STMD neurons (e.g. robustness against background texture) it was implemented using computationally intensive continuous-time processing. A major goal of the present paper was to implement the key elements of this model using industry-standard discrete-time simulation tools, thus opening up practical applications of the model for real-time, closed loop simulations or robotics. In addition, we describe the application of a more physiologically accurate log-normal filter in place of first order filter approximations, the addition of a Reichardt Correlator to the ESTMD outputs in order to implement direction selectivity, and the results of testing the algorithm in a virtual world implemented using Simulink.

II. Modifications to Detection Algorithm

A. Overview of Digital Implementation

Our previous target-detection algorithms were constructed for the purpose of investigating underlying physiological mechanisms, rather than for the development of robotic systems [6, 7]. The benefit of the continuous domain in this instance is that it provides a good coherence to physiological occurrences, and is thus applicable to mimicking physiology [8]. To improve applicability of the detection algorithms to situations involving hardware however, the algorithms must be re-coded within the discrete domain. This involves the identification of all temporal filters, and subsequent conversion into the discrete domain. A model overview of the algorithms proposed by the authors is shown in Figure 1. The

algorithms are effectively categorised into five sections; Fly Optics, Photoreceptors (PRs), Large Monopolar Cells (LMCs), Rectifying Transient Cells (RTCs) and the final output.

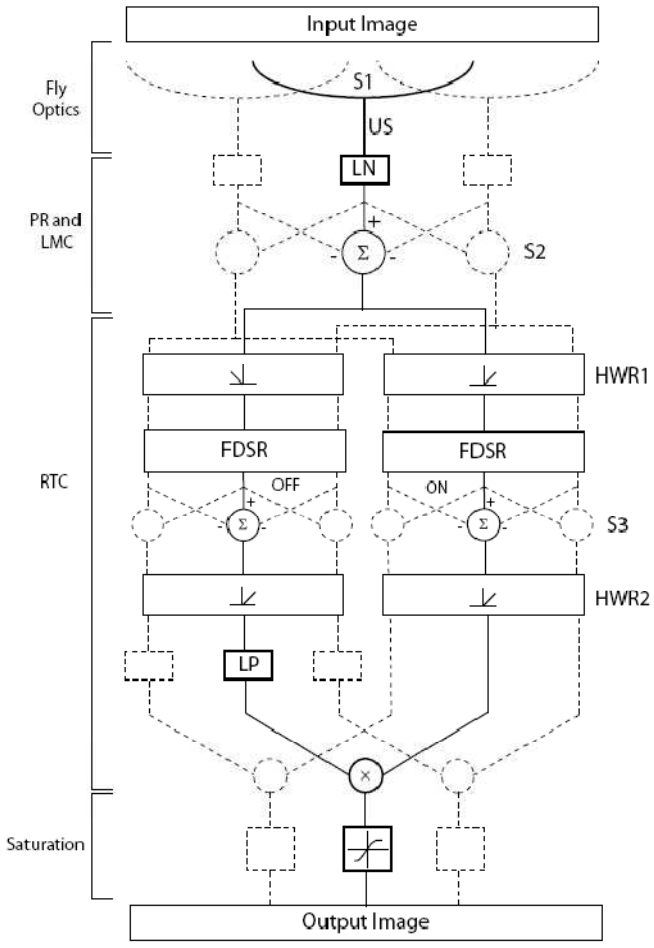

Fig. 1- Detailed model overview. Fly Optics includes spatial image filtering (S1) followed by under-sampling (US). The Photoreceptors (PR) and Large Monopolar Cells (LMC) then temporally filter the image using a log-normal filter (LN), followed by spatial image filtering (S2). The image is split into independent channels corresponding to contrast increments (ON channel) and contrast decrements (OFF channel) in the Rectifying Transient Cell (RTC), through half-wave rectification of the signal (HWR1). The channels are filtered separately through Fast Depolarising – Slow Repolarising (FDSR) inhibition, then spatially filtered with stronger surround inhibition (S3). Following this the image is half-wave rectified (HWR2) to remove negative components, then the OFF channel is delayed through a low pass filter (LP) and recombined in a quadratic manner (X). Following this non-linear saturation of the image occurs.

B. Pre-filtering

Prior to any motion or flicker detection in the image, it is spatially and temporally filtered through the 'Fly Optics', 'PRs' and 'LMCs'. Fly Optics refers to the blurring and under-sampling (S1 and US respectively in Figure 1) of the green colour channel of the image, which is used so as to approximate the spectral sensitivity of fly photoreceptors [9]. This is implemented through the application of a Gaussian convolution mask, with a full width at half maximum of 1.4°, followed by spatial under sampling at 1° separation to mimic the resolution of the fly eye [6]. The resulting data is then passed through the PR and LMC sections of the algorithms.

It is known that the response of a fly photoreceptor is temporally limited, in that there is a slight delay in the response to stimuli with a corner frequency of 40-70Hz [10]. While the LMC's have been shown to remove redundant information [11] by acting as a spatiotemporal contrast detector. In order to reduce processing time, we have combined the low pass temporal filter of the PR's and the temporal component of the LMC into one temporal band pass filter (LN in Figure 1). Such an action leads to the same output as when the filters are separated, since both are linear. This action is supported by research, which suggests that such a band pass filter could be represented in a physiologically accurate manner by a difference of log-normals model [12]. James [13] created such a log-normal model which provides a good fit to the temporal impulse response at the LMC. The impulse response of this log-normal function is shown in Figure 2 in red. Using MATLAB an approximation of this response in the form of a discrete transfer function can be found. As can be seen in Figure 2 in blue, the approximation is accurate, with a sampling rate of 1000Hz.

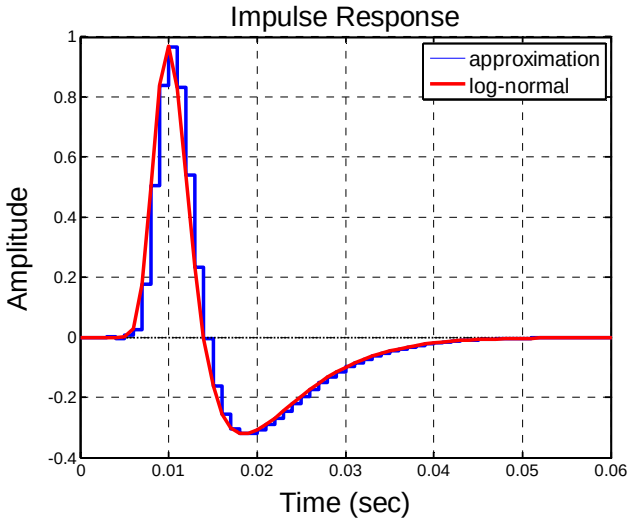

Fig. 2- Impulse response of the log-normal model [13] of Photoreceptor and LMC temporal filtering characteristics (red line), and a discrete filter approximation (blue line).

The transfer function describing the continuous filter shown in Figure 2 is given by Equation (1), while that of the discrete approximation is given by Equation (2).

$$G(t) = 1.06\, exp^{\left(\left(-\log_{10}\frac{t}{0.505}\right)^2/0.0776\right)} - 0.3356\, exp^{\left(\left(-\log_{10}\frac{t}{0.875}\right)^2/0.238\right)} \quad (1)$$

$$G(z) = \left(\begin{matrix}0.00006z^7 - 0.00076z^6 + 0.0044z^5 - 0.016z^4 \ldots \\ + 0.043z^3 - 0.057z^2 + 0.1789z - 0.1524\end{matrix}\right) \times \left(\begin{matrix}z^8 - 4.333z^7 + 8.685z^6 - 10.71z^5 + 9z^4 \ldots \\ - 5.306z^3 + 2.145z^2 - 0.5418z + 0.0651\end{matrix}\right)^{-1} \quad (2)$$

A further convolution mask effectively acting as a spatial band pass filter is applied to the image in order to accentuate edges (S2 in Figure 1); this represents the spatial component of the LMC. The spatial filter is implemented by convolving the image with a kernel which effectively applies a negative weighting to the pixels surrounding each and every pixel, thus inducing 'centre-surround antagonism' of the image. The kernel is given by

$$H = \begin{bmatrix} -1/9 & -1/9 & -1/9 \\ -1/9 & 8/9 & -1/9 \\ -1/9 & -1/9 & -1/9 \end{bmatrix}. \quad (3)$$

In contrast to our previous research, this kernel was made a zero mean filter, as opposed to a 10% surround (as a percentage of the centre pixel) in order to provide a zero DC response. The effect of this change is discussed in Section IV.

C. Local Flicker Detection

The Rectifying Transient Cell (RTC) is a method of detecting localized flicker. When used in conjunction with the previous filters, the RTC is apt at detecting object motion [6]. Following the LMC filtering, the image signal is composed of a range of both positive and negative values, due to the spatial band pass filtering. The RTC [6] separates these positive and negative parts (or 'ON' and 'OFF' channels respectively) through half-wave rectification (HWR1 in Figure 1), and inverts the sign of the negative phase. Each independent channel of the RTC is then formed into an 'adaption state' through the application of a non-linear low pass filter with a fast depolarizing, slow repolarizing characteristic [6], such that inputs with a positive contrast gradient are subjected to a fast filter, while signals with a negative contrast gradient undergo slow low pass filtering. The filtered signal is then subtracted from the un-filtered signal. This process serves to inhibit recurring 'bursty' inputs, such as noise. This process is shown as FDSR in Figure 1, though is expanded as shown in Figure 3.

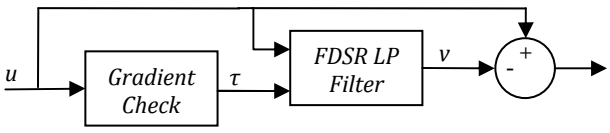

Fig. 3- FDSR algorithm. The input image '*u*', following halfwave rectification, is fed into the 'Gradient Check' block, which determines whether the luminance of each individual pixel is rising or falling, and outputs a matrix of appropriate '*τ*' (time constant) values. Both '*u*' and '*τ*' are fed into the FDSR low-pass filter block, which filters each pixel of the image according to the time constant value, and outputs the filtered image '*v*', which is then subtracted from the original image '*u*'. This computation emulates fast temporal adaptation, reducing responses to textural variations in the image.

In digital form the application of the 'Gradient Check' (seen in Figure 3) in this process caused much difficulty, as the digital signal does not have a continuous derivative, thus the gradient of the signals must be found through comparative analysis of transient signals rather than computed directly. Also, to enable dynamic adjustment of the low-pass filter (FDSR LP Filter in Figure 3) time constants for each individual pixel (1ms for the fast filter, 100ms for the slow filter) in the Simulink environment, a state space representation of the filter had to be used, and can be seen in Figure 4.

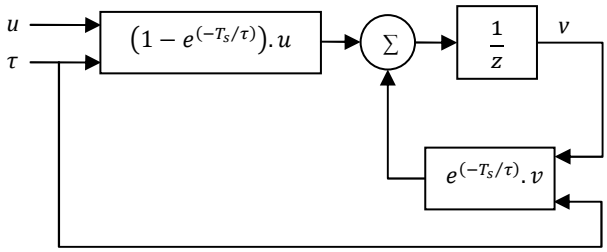

Fig. 4- Block diagram showing the FDSR low pass filter. Here, '*u*' is the input image following half wave rectification, '*τ*' is the time constant which is dynamically changing, 'T_s' is the sampling time in seconds and '*v*' is the output of the filter, which is then subtracted from the direct feed-through version of u.

Each of the separated phases then undergo further centre-surround antagonism, where surrounding ON channels subtractively inhibit the centre ON channel and similarly for the OFF channels. This is implemented through the application of a spatial band-pass filter convolution mask to each of the channels, as in the LMC phase, though with a stronger surround inhibition (S3 in Figure 1). This strong surround inhibition helps to selectively tune the model to small sized targets. The kernel used in this convolution is given by

$$H = \begin{bmatrix} -1 & -1 & -1 & -1 & -1 \\ -1 & 0 & 0 & 0 & -1 \\ -1 & 0 & 2 & 0 & -1 \\ -1 & 0 & 0 & 0 & -1 \\ -1 & -1 & -1 & -1 & -1 \end{bmatrix}. \quad (4)$$

Following the application of a convolution mask, both channels are again half-wave rectified in order to remove any negative data (HWR2 in Figure 1). At this stage, an ON channel graphically refers to a spatiotemporal transition from low to high luminance level (i.e. black to white), whereas an OFF channel refers to a high to low transition.

Following this, the OFF channel is delayed and multiplied by the un-delayed ON channel. Delaying of the OFF channel is achieved through the use of a first order low pass filter (LP in Figure 1), the time constant of which is chosen to further determine the velocity and size tuning of the model. Tuning for an arbitrary target size of one pixel, the low pass filter has a time constant of 25ms, which, for a first order low pass filter gives a transfer function of

$$G(s) = \frac{1}{0.025s + 1}. \quad (5)$$

Using Tustin's Method for approximation of a digital filter [14] with a sampling time of 0.001 seconds, the digital transfer function for this filter is found to be

$$G(z) = \frac{z+1}{51z-49}. \quad (6)$$

The filter is applied over each pixel in the OFF channel individually, and the result is multiplied on a pixel-by-pixel basis by the un-delayed ON channel.

The image then undergoes non-linear saturation using the hyperbolic tan function, to ensure all signals lie between 0 and 1, and thresholding to rid the output of anomalies. The algorithms have been found to act as an effective matched pre-filter for target selectivity, which produces data that is well-suited to feed into higher order target extraction mechanisms. As the algorithms are tuned to specific sizes and velocities, it is of interest to examine their response to other stimuli, and under complex and possibly confounding conditions, this will be discussed in Section IV.

D. Reichardt Correlator

While the ESTMD model of Wiederman et al. [6, 7] is insensitive to direction of motion, some STMD neurons respond selectively depending on the direction of motion of a target. One model which has been proposed which explains the ability of neurons to detect motion and direction of an object is the correlation method [15]. The correlation method, first proposed by Hassenstein and Reichardt with the Reichardt Correlator [15], determines if motion has occurred in an image through the spatiotemporal correlation of luminance signals of neighbouring points in an image. If an object moves past two sequential points on an image, then the signal from the object at the second point will be a time-shifted version of the object at the first point, where the time-shift, or delay, is the time taken for the object to move from one point to the next [15]. Multiplying these two signals produces an output which indicates motion of the object, and is tuned to an optimum speed dependent on the amount of delay time [16]. This model can be extended to detect motion in the opposite direction by mirroring the model, producing a second output. Through subtraction of the two outputs, direction of movement can also be determined, in that movement one direction will cause a positive output, while movement in the opposite direction will cause a negative output.

Thus, the application of a Reichardt Correlator to the image, following analysis by the detection algorithms, provides a method of detecting the direction of motion of a target in a computationally efficient manner. The Reichardt Correlator may be implemented in the digital form of the model by multiplying each pixel by a delayed version of each of its neighbouring pixels, producing both vertical and horizontal motion detectors.

III. VIRTUAL WORLD

In order to test the detection algorithm under realistic, simulated conditions, a virtual world (Figure 4) was created using the Simulink 3D Animation toolbox [17], which enables the user to adjust aspects of the world, including the position and rotation of objects, during simulation in response to external stimuli. Previously [7], the detection algorithms have been tested by rotating a High Dynamic Range (HDR) panorama, with pseudo-embedded black targets, past the model input, meaning that there were no relative motion cues between the target and background. The use of a virtual world to test the algorithms enables the introduction of relative motion cues between the target and background, by making them separate objects. This relative motion can be adjusted as well in order to increase the difficulty of object tracking, and thus determine the point at which the model breaks down.

In order to make the visual feed more realistic, a high resolution image of the users choice can be rendered on the background of the world, thus, as the pursuer flies closer to the background (mapped in the VR world as a hollow cylinder within which the target and pursuer fly) the detail of the image increases as the image is 'zoomed in' on. These natural images are of sufficient complexity to provide a level of difficulty in discerning the target.

It has been shown that natural scenes display the consistent statistical property of a $1/f^2$ relationship between spatial frequency and power [18]. Thus, in order to present the closest representation of a natural scene as possible, inputs to the bio-mimetic model must follow this relationship. Thus, the input to the model is an 8 bit panoramic image of a natural scene, displaying natural image statistics. Though such an image is likely to be large in terms of size and required processing capabilities, it is important to emulate the real situation in order to determine if the model produces an output imitating that of the experimental results, or conversely, where the model breaks.

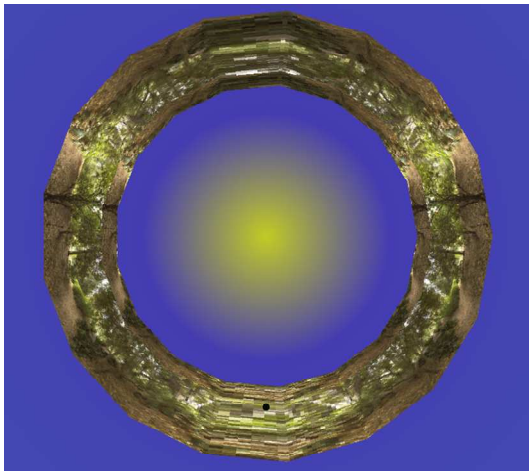

Fig. 4- Top view of virtual world. In this image the target can be seen against the lower section of the cylinder. The viewpoint would be situated at the centre of the cylinder, facing a wall.

IV. MODEL PERFORMANCE

The purpose of our new implementation of the model was to successfully mimic the behaviour of the continuous model created by Wiederman et al [6], which was based upon

physiological data, as well as the testing of the model under more generalised stimuli through the use of the virtual world input. A successful digital implementation may have future uses in hardware systems, and is thus a worthwhile endeavour. Implementing this code in Simulink makes the targeting of specific hardware, for example Field Programmable Gate Arrays (FPGAs) relatively simple. This is due to the fact that Simulink code may be easily re-written in HDL, and is thus able to be integrated into an FPGA.

This section will discuss in depth the similarity of the digital model response under the same conditions imposed on the continuous model.

A. Response to Target Size

As has been previously stated, the model is tuned to respond optimally to small sized targets by spatial band pass filtering, in particular the filter S3 in Figure 1. In the previous model [6], the authors aimed to produce a velocity tuned output similar to the physiological phenomenon. The aim of the current implementation however, is to produce a velocity tuned output from a digital model, similar to that produced by the continuous model. This similarity was tested by recording the response of the algorithms to different sized targets under the same conditions as those used to test the continuous algorithms [6]. The response of the algorithms under such conditions is important to know for future applications of the model, such as pursuit. As such, the model was presented with a black target moving at a constant velocity against a white background. The response to the target was recorded as the height of the object was changed (the width was held constant at 0.8°). The results of this test can be seen in Figure 5a, overlayed on the results of the same test for the continuous model [6].

It can be seen that both models display similar responses to a change in target height, with both curves being very similar in shape, though the digital implementation of the algorithms produces a left shifted version of the curve. This difference is expected, as discussed earlier, as the kernels involved in spatial convolution of the data in the LMC stage of processing have differing surrounding elements. It is thus clear that by increasing the surround antagonism imposed by these elements, that the model may be tuned to differing target sizes. This shift in results is of small consequence however, as the aim of the current implementation was to re-produce the specific size tuning behaviour of the continuous model [6], and it can be clearly seen that the discrete implementation closely mimics the tuning curve shape, and thus the continuous models size tuning behaviour.

B. Response to Target Velocity

Future applications of the detection algorithms, such as the inclusion in pursuit activity, may rely on the model continuing to work under varied target velocities. As such, the response characteristics of the model to varied target velocities must be analysed. For the digital implementation of the model to be deemed a success, it should display similar characteristics to

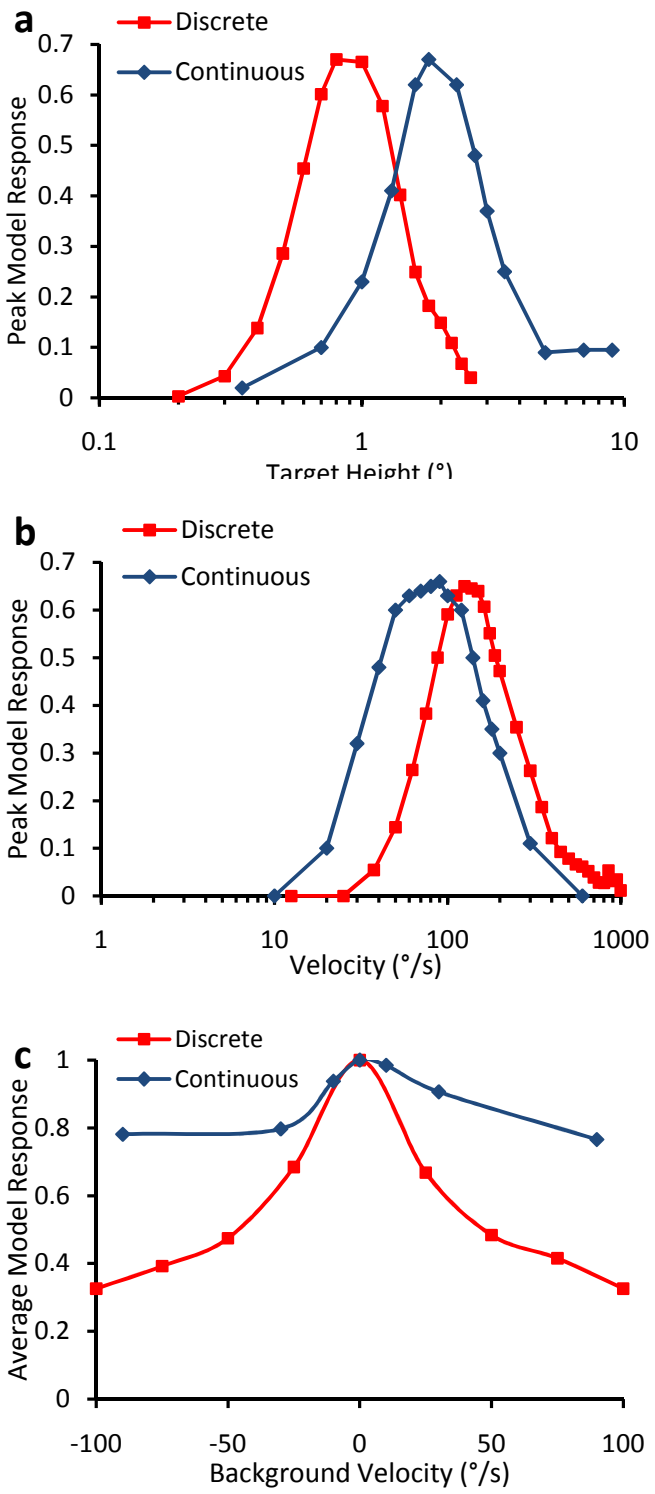

Fig. 5 – Model Tuning. (a) The maximum response of both a discrete and continuous model to changes in height of a black target (of constant velocity 50°/s velocity) while width is kept constant at 0.8°, against a white background. (b) The maximum response of both models to changes in velocity of a black target (of constant size 0.8° x 0.8°) against a white background. (c) The average response of both a discrete and continuous model to a black target (of constant size 0.8° x 0.8°, and velocity 90°/s) against natural image background of changing velocity. Results of the continuous model were obtained from [6].

those shown by the continuous model [6]. Thus the response of the digital model with various target sizes can be seen in Figure 5b overlayed on the results of the continuous model under the same conditions. These conditions were a constant target size of 0.8° x 0.8°.

Again, both models display similar responses to the change in target velocity, though the continuous model is optimally tuned to a slightly higher band of velocities. Tuning of the model to certain velocities is achieved solely by the RTC component of the detection algorithm; in particular the low pass filter, LP, delaying the OFF channel prior to multiplication with the ON channel. As such, a slower low pass filter would tune the model to slower targets; conversely, a faster filter would tune the model to faster targets. Thus, to more accurately represent the continuous model, one could slow the low pass filter, though for use in hardware implementation, this would need to be set to optimally suit the requirements.

C. Response to Background Velocity

The current method of implementation of the discrete model, involving the use of a virtual world as an input, enables the testing of the model under varied stimuli. One such application of the model is under the more realistic situation of relative motion between the target and the background. Again, the success of the digital implementation of the model is dependent on the similarity of results between the continuous model [6] and the discrete model. As such, the response of the discrete model to the motion of a black target against a natural scene, where the velocities of the scene and target are not necessarily the same, must be analysed. This was achieved by maintaining a constant target velocity, 90°/s, and altering the background velocity, at a range of starting positions on the image. Hence, at a background velocity of 90°/s, there is no relative motion between the target and background. This can be seen in Figure 5c.

It can be seen from Figure 5c that the curves of both the discrete and continuous model are similar in shape, in that the response reaches a maximum when the background speed approaches zero. It is evident that the continuous model appears to be more robust under the presence of background motion. This is an intriguing difference in the results which is not related to thresholding or normalisation of the output. This difference may be due to numerous factors, including differences in background images and target positions, spatial kernels, or various other model distinctions. As the analysis of the effect of background velocity is a significant factor of the virtual world implementation, it is great interest in future research to perform a sensitivity analysis on this finding.

V. Conclusions and Future Work

The progress made on the biologically inspired detection algorithms includes the implementation of the algorithm in digital space, the application of the more physiologically accurate log-normal filter, the addition of a Reichardt Correlator, and the results of testing the algorithm in a virtual world. This progress has led to the creation of digital algorithms which display similar tuning characteristics to the continuous model. With the addition of the virtual world input to the model, more generalised simulations have been made possible, and due to the discrete temporal nature of the algorithms, hardware (FPGA) implementation is foreseeable. It is expected that through the implementation of a feedback control system, the algorithms could be employed in a pursuit situation of small moving targets.

Acknowledgements

This research was supported by the US Air Force Office of Scientific Research (FA 2386-10-1-4114).
Panoramic Image Courtesy of Dr Russell Brinkworth.

References

[1] S. Shaw, “Early Visual Processing in Insects,” *J Exp Biol* , vol. 112, pp. 225 - 251, 1984.
[2] K. Nordstrom, D. O’Carroll, “Feature Detection and the Hypercomplex Property in Insects,” *Trends Neurosci*, vol. 32, no. 7, pp 383-391, 2009.
[3] T. Collett, “Visual Control of Flight Behaviour in the Hoverfly,” *J Comp Physiol*, vol. 99, no. 1, pp. 1-66, 1975.
[4] K. Nordstrom, P. Barnett, and D. O'Carroll, “Insect Detection of Small Targets Moving in Visual Clutter,” *PloS Biol* , vol. 4, no. 3, pp. 1-9, 2006.
[5] Y. Ren, C. Chua, and Y. Ho, “Motion detection with nonstationary background,” *Mach Vision Appl*, vol. 13, no. 5, pp. 332-343, 2003.
[6] S. Wiederman, P. Shoemaker, and D. O'Carroll, “A Model For the Detection of Moving Targets in Visual Clutter Inspired by Insect Physiology,” *PLoS ONE* , vol. 3, no. 7, pp. 1-11, 2008.
[7] S. Wiederman, R. Brinkworth, and D. O'Carroll, “Performance of a Bio-Inspired Model for the Robust Detection of Moving Targets in High Dynamic Range Natural Scenes,” *J Comput Theor Nanos* , vol. 7, no. 5, pp. 1-10, 2010.
[8] J.H. van Hateren and H.P. Snippe, “Information Theoretical Evaluation of Parametric Models of Gain Control in Blowfly Photoreceptor cells,” *Vision Res*, vol. 41, pp. 1851-1865, 2001.
[9] M.V. Srinivasan, RG. Guy, “Spectral properties of movement perception in the dronefly Eristalis,” *J Comp Physiol A*, vol. 166, pp. 287–295, 1990.
[10] S. Laughlin, and M. Weckstrom, “Fast and Slow Photoreceptors - A Comparative Study of the Functional Diversity of Coding and Conductances in Diptera,” *J Comp Physiol*, vol. 172, no. 5, pp. 593-603, 1993.
[11] P. Coombe, M. Srinivasan, and R. Guy, “Are the Large Monopolar Cells of the Insect Lamina on the Optomotor Pathway?,” *J Comp Physiol*, vol. 166, no. 1, pp. 23-35, 1989.
[12] R. Payne, J. Howard, “Response of an Insect Photoreceptor: A Simple Log-Normal Model,” *Nature*, vol. 290, pp. 415-416, 1981.
[13] A. James, “White Noise Studies in the Fly Lamina,” PhD Thesis, Australian National University, Canberra, Australia, 1990.
[14] E.C. Ifeachor, BW. Jervis, *Digital Signal Processing – A Practical Approach*, 2nd ed., New York: Prentice Hall, 2002.
[15] A. Derrington, L. Delicato, H. Allen, “Visual Mechanisms of Motion Analysis and Motion Perception,” *Annu Rev Physiol* , vol. 55, pp. 181-205, 2003.
[16] B. Hassenstein, W. Reichardt, “Systemtheoretische Analyse der Zeit-Reihenfolgen- und Vorzeichenauswertung bei der Bewegungsperzeption des RÄusselkÄafers Chlorophanus,” *Z. Naturforsch.*, pp. 513-524, 1956.
[17] (2011), The MathWorks website. [Online]. Available: http://www.mathworks.com/fpga-design/index.html.
[18] D. Field, “Relations Between the Statistics of Natural Images and the Response Properties of Cortical Cells,” *OSA Proc*, vol. 4, no. 12, pp. 2379-2394, 1987.